AU J.T. 14(4): 243-252 (Apr. 2011)

Development and Design of Constant-Force Compression Spring Electrical Contacts

Ikechukwu Celestine Ugwuoke

Department of Mechanical Engineering, Federal University of Technology Minna, Niger State, Nigeria
E-mail: <ugwuokeikechukwu@yahoo.com>

Abstract

This research focused on the development of modified configurations of compliant constant-force mechanisms (CCFMs) for use as constant-force compression spring electrical contacts (CFCSECs). These new configurations promise to create new possibilities in the design of electrical contacts (ECs), possibilities in lowering required manufacturing tolerances, reduction of system sensitivity to variations introduced during usage, increased system robustness in applications where movement and/or vibrations exist and will also go a long way in overcoming the challenges encountered in the implementation of the current traditional CCFMs in ECs. The successful development of CFCSECs that meets all of the requirements of an EC will lay a ground work for further exploration and introduction of CFCSECs into industry applications. These new configurations have successfully eliminated all pin joints and have replaced them with short flexural pivots, and where these short flexural pivots exist, they only serve to mimic the local hinges. The results show that CFCSECs demonstrated substantially constant output force over the range of its input displacement.

Keywords: *compliant constant-force mechanisms, constant-force compression spring electrical contacts, manufacturing tolerances, system sensitivity, system robustness.*

1. Introduction

The reliability of electrical contacts (ECs) is of great concern to most designers, and several methods are being developed to improve said reliability (Harper 1996). Studies have shown that 85% of all automotive electrical problems are a result of contact integrity problems. Also, over 70% of all computer hardware problems can be traced back to contact problems. To maintain contact integrity in practice, ECs must transmit electrical signal with minimal contact resistance under all types of usage conditions and must also accommodate expected variations in geometry during manufacture and assembly. Two physical parameters that greatly affect contact integrity are the contact surface finish and the contact normal force at mating. When the contact surface finish remains corrosion free, contact integrity is maintained. Also, when the contact normal force is kept above a certain level, contact integrity is also maintained. Thus a desirable EC would maintain an optimal contact force regardless of variations during assembly or usage. Compliant mechanisms (CMs) are single-piece flexible structures that use strain energy to transform input energy components into a desired output force or displacement. They can be manufactured via injection moulding, extrusion and rapid prototyping for medium size devices (Mortensen *et al*. 2000) or using silicon surface micromachining (Larsen *et al*. 1997) and electroplating techniques (Chen 2001) for micro-mechanisms. Although a CM gives numerous advantages, it is difficult to be designed and analyzed. The current traditional compliant constant-force mechanism (CCFM) configurations are not suitable for use as ECs for several different reasons which include (Weight 2001):

1) Manufacturability - The stamping of the necessary geometry would be difficult.
2) Material - The deflections and size constraints would cause extremely high stresses compared to the strengths of common electrical contact materials.
3) Assembly - The assembly of pin-joints makes the use of traditional slider-crank configurations in electrical contacts unlikely.
4) Electrical Continuity - Pin joints would introduce gaps and areas of high resistance in the electrical path making the contact inefficient and unreliable.

This research focused on the development of modified configurations of CCFMs for use as constant-force compression spring electrical contacts (CFCSECs). These new configurations promises to create new possibilities in the design of ECs, possibilities in lowering required manufacturing tolerances, reduction of system sensitivity to variations introduced during usage, increased system robustness in applications where movement and/or vibrations exist, and will also go a long way in overcoming the challenges encountered in the implementation of the current traditional CCFMs in ECs. The successful development of CFCSECs that meets all of the requirements of an EC will lay a ground work for further exploration and introduction of CFCSECs into industry applications which is a large step forward.

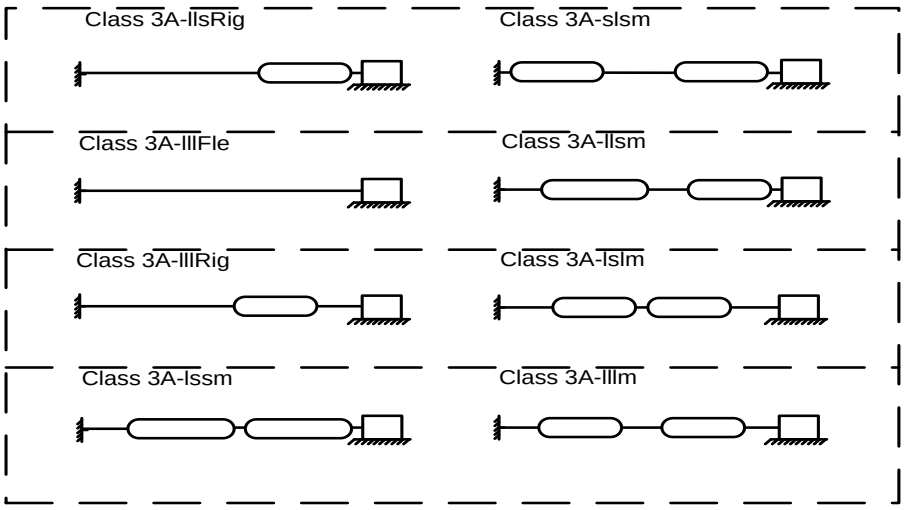

Fig. 1. Developed configurations of CFCSECs.

Unlike regular linear springs which yield an increased force with increase displacement, CFCSECs combine the effects of mechanical advantage and stored strain energy of flexible members to obtain a constant output force over a large range of displacements. CFCSECs can be fabricated from any conductive material. Current industry practice is to use alloys that contain copper. Phosphor bronze is a common alloy that is easy to use and readily available and it is capable of withstanding repeated flexures. It is commonly used in electrical components because of its good electrical properties and resistance to corrosion. It is also suitable to be used in sub-zero temperatures and generally will not change dimensions under heat. Beryllium copper and titanium copper are commonly used to achieve higher yield strengths. Unfortunately, they are more difficult to use and more expensive than phosphor bronze. Figure 1 shows the developed configurations of CFCSECs. As shown in Fig. 1, these new configurations have successfully eliminated all pin joints and have replaced them with short flexural pivots, and where these short flexural pivots exist, they only serve to mimic (simulate the behavior of) the local hinges.

2. Design Analysis

2.1 Pseudo-Rigid-Body Model Formulation

Figure 2 shows the generalized pseudo-rigid-body model (GPRBM) simplification for all configurations of CFCSECs. Tables 1, 2 and 3 give the length parameter formulas and values, the spring constant formulas, and the needed values to calculate the flexible and rigid segment lengths as defined in Fig. 3, respectively, for the different configurations of CFCSECs.

The following expressions, together with those tabulated in Table 2, may be used to determine the length of the flexible and rigid segments for the different CFCSECs:

$$r_{Tot} = \frac{L_{Tot}}{\lambda}, \quad (1)$$

$$r_{Tot} = r_2 + r_3 = \text{Total PRBM length}, \quad (2)$$

$$R = \frac{r_3}{r_2} = \text{Geometric parameter ratio}, \quad (3)$$

$$r_2 = \frac{r_{Tot}}{(R+1)}, \quad (4)$$

$$r_3 = \frac{r_{Tot}}{\left(\frac{1}{R}+1\right)}, \quad (5)$$

L_{Tot} = Total length of actual CFCSEC.

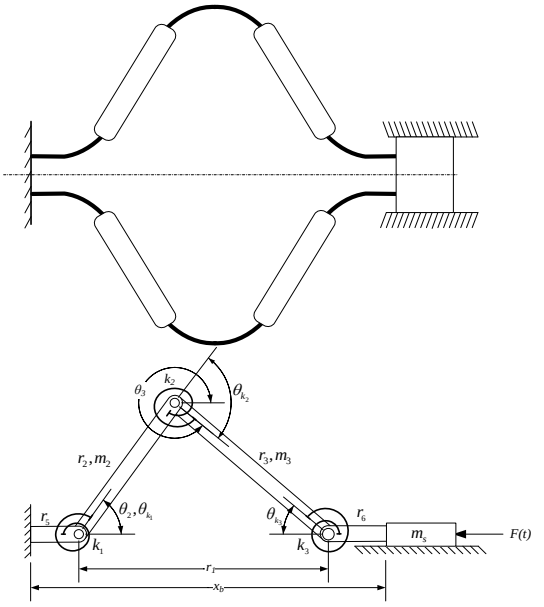

Fig. 2. *Class 3A-lllm* CFCSEC configuration, and the GPRBM for all CFCSEC configurations.

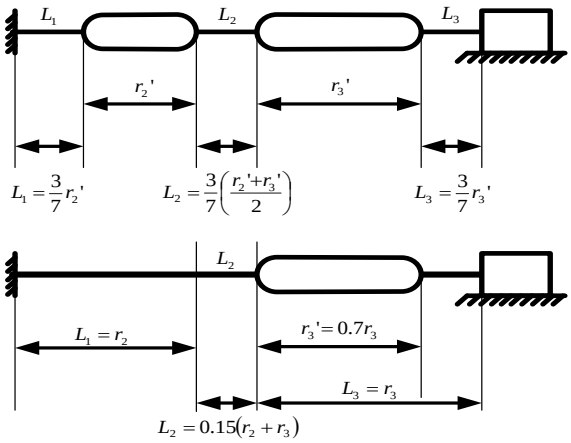

Fig. 3. Definition of flexible and rigid segment lengths.

Table 1. Length parameter formulas and values for CFCSECs.

Configuration	Length Parameter λ Formula	λ values	R values
Class $3A-lssm$	$(0.886R+0.996)/(\gamma(R+1))$	1.1071	1.0000
Class $3A-slsm$	$(1.04R+1.04)/(R+1)$	1.0400	1.0000
Class $3A-llsm$	$(0.986R+0.874)/(\gamma(R+1))$	1.0941	1.0000
Class $3A-lslm$	$(0.994R+0.994)/(\gamma(R+1))$	1.1694	1.0000
Class $3A-lllm$	$(1.15R+1.15)/(R+1)$	1.1500	1.0000
Class $3A-llsRig$	$(1.02R\gamma+1)/(\gamma(R+1))$	1.0960	1.0000
Class $3A-lllFle$	$(1.15R+1.15)/(R+1)$	1.1500	1.0000
Class $3A-lllRig$	$(1.15R+1.15)/(R+1)$	1.1500	1.0000

Table 2. Spring constant formulas for CFCSECs.

Configuration	k_1	k_2	k_3
Class $3A-lssm$	$0.3\gamma K_\theta EI/L_1$	EI/L_2	EI/L_3
Class $3A-slsm$	EI/L_1	$0.3\gamma K_\theta EI/L_2$	EI/L_3
Class $3A-llsm$	$0.6\gamma K_\theta EI/L_1$	$0.3\gamma K_\theta EI/L_2$	EI/L_3
Class $3A-lslm$	$0.3\gamma K_\theta EI/L_1$	EI/L_2	$0.3\gamma K_\theta EI/L_3$
Class $3A-lllm$	$0.6\gamma K_\theta EI/L_1$	$0.6\gamma K_\theta EI/L_2$	$0.6\gamma K_\theta EI/L_3$
Class $3A-llsRig$	$2\gamma K_\theta EI/L_1$	$\gamma K_\theta EI/L_2$	EI/L_3
Class $3A-lllFle$	$2\gamma K_\theta EI/L_1$	$2\gamma K_\theta EI/L_2$	$2\gamma K_\theta EI/L_3$
Class $3A-lllRig$	$2\gamma K_\theta EI/L_1$	$2\gamma K_\theta EI/L_2$	$2\gamma K_\theta EI/L_3$

Table 3. Flexible and rigid segment lengths for CFCSECs.

To get:	L_1	L_2	L_3	r_2'	r_3'
Configuration	Multiply r_2' by	Multiply r_{ave}' by	Multiply r_3' by	Subtract from r_2	Subtract from r_3
Class $3A-lssm$	$3/7$	0.1	0.1	$0.5(L_1+L_2)$	$0.5(L_2+L_3)$
Class $3A-slsm$	0.1	$3/7$	0.1	$0.5(L_1+L_2)$	$0.5(L_2+L_3)$
Class $3A-llsm$	$3/7$	$3/7$	0.1	$0.5(L_1+L_2)$	$0.5(L_2+L_3)$
Class $3A-lslm$	$3/7$	0.1	$3/7$	$0.5(L_1+L_2)$	$0.5(L_2+L_3)$
Class $3A-lllm$	$3/7$	$3/7$	$3/7$	$0.5(L_1+L_2)$	$0.5(L_2+L_3)$
Class $3A-llsRig$	$\frac{(0.85r_2-0.14r_3)}{0.7225}$	$1/0.88(\times r_3)$	0.1	r_2	$0.15L_2+0.5L_3$
Class $3A-lllFle$	r_2	$0.15(r_2+r_3)$	r_3	r_2	r_3
Class $3A-lllRig$	r_2	$0.15(r_2+r_3)$	r_3	r_2	$0.15(L_2+L_3)$

2.2 Behavioral Model Formulation Using the Principle of Virtual Work Analysis

The concept of virtual work is a very useful device for solving both static and quasi-static force-analysis problems. Virtual work, however, refers to imagined work, the displacement does not actually occur, it is introduced as an imagined quantity (Sandor and Erdman 1988). A mechanism with rigid components is in a state of static equilibrium if the sum of the virtual work done by all real forces and moments is zero for every virtual displacement consistent with the kinematics constraints. If elastic components are a part of the mechanical system, the total virtual work done by these elastic components is equal to the total virtual work of all real forces and moments (acting on the non elastic components) for virtual displacement consistent with the constraint (Sandor and Erdman 1988). Thus, for such a system:

$$\sum_P (F_i \bullet \delta s_i) + \sum_P (M_i \bullet \delta\phi_i) + \sum_Q (R_j \bullet \delta s_j) + \sum_Q (T_j \bullet \delta\phi_j) = \sum_S (E_k \bullet \delta s_k) + \sum_S (K_k \bullet \delta\phi_k), \qquad (6)$$

where:

F_i = active force vector at i;
M_i = active moment vector at i;
$i = 1, 2, \ldots, P$ is the point of application;
R_j = reactive force vector at j;
T_j = reactive moment vector at j;
$j = 1, 2, \ldots, Q$ is the point of reaction;

E_k = elastic force resultant in resilient connector k;

K_k = elastic moment resultant in resilient connector k;

$k = 1, 2, \ldots, S$ is the point of attachment;

δs_k, $\delta \phi_k$ = virtual deflections of resilient connectors.

Friction and inertia forces can be easily added as forces and moments. Application of the principle of virtual work to the GPRBM of CFCSECs and taking θ_2 as the generalized coordinate gives the following expression:

$$F_{VW} = \frac{k_1}{r_2\left(\frac{r_3}{r_2}\right)\sin(\theta_2-\theta_3)}\left(\left(\frac{r_3}{r_2}\right)\theta_{k1}\cos\theta_3 + \left(\frac{k_2}{k_1}\right)\theta_{k2}\left(\cos\theta_2+\left(\frac{r_3}{r_2}\right)\cos\theta_3\right) + \left(\frac{k_3}{k_1}\right)\theta_{k3}\cos\theta_2\right) \quad (7)$$

Equation (7) tells how the force F_{VW} is related to the link lengths, spring constants, and angles of the CFCSEC. Inspection of Eq. (7) shows that it relies on many independent variables. It is beneficial to generalize the model in order to simplify its use. One method to do this is to try and replace all independent variables with dimensionless parameters. In the complimentary work done by Millar *et al*. (1996) and Weight (2001), three non-dimensionaliszed parameters R, K_1 and K_2 were chosen. These parameters, when substituted into Eq. (7) give the expression below:

$$F_{VW} = \frac{k_1}{r_2 R\sin(\theta_2-\theta_3)}\left(R\cos\theta_3\left(\theta_{k1}+K_1\theta_{k2}\right) + \cos\theta_2\left(K_1\theta_{k2}+K_2\theta_{k3}\right)\right), \quad (8)$$

where:

$$K_1 = \frac{k_2}{k_1} \text{ and } K_2 = \frac{k_3}{k_1}. \quad (9)$$

Because CFCSECs, as presented in Fig. 1, contain no rigid joints, their operation is friction free, with no backlash or wear. Associated with the CFCSEC's links/segments are:

1) Possible flexing of the rigid links of CFCSECs; and
2) Possible flexing of the portion of the compliant segments that was assumed to be rigid.

These possibilities are compensated for by introducing the term M_{AFE} (moment due to axial force effects). Moment M_{AFE} may be approximated using the expression

$$M_{AFE} = F_{VW}\delta e = F_{VW} r_2 \alpha_{AFE}\left(1+\frac{r_2}{r_3}\right), \quad (10)$$

where α_{AFE} is the angle of axial force effect.

Moment M_{AFE} is transformed to force F_{AFE} using the power relationship given as:

$$F_{AFE}\dot{r}_1 = F_{AFE}\dot{\theta}_2\left(\frac{\partial r_1}{\partial \theta_2}\right) = -r_2\sin\theta_2\left(1+\frac{r_2\cos\theta_2}{\sqrt{r_3^2-r_2^2\sin^2\theta_2}}\right)\dot{\theta}_2 \times F_{AFE} = M_{AFE}\dot{\theta}_2, \quad (11)$$

$$M_{AFE} = -r_2\sin\theta_2\left(1+\frac{r_2\cos\theta_2}{\sqrt{r_3^2-r_2^2\sin^2\theta_2}}\right)\times F_{AFE}, \quad (12)$$

$$M_{AFE} = F_{VW} r_2 \alpha_{AFE}\left(\frac{R+1}{R}\right) = -r_2\sin\theta_2\left(1+\frac{\cos\theta_2}{\sqrt{R^2-\sin^2\theta_2}}\right)\times F_{AFE}, \quad (13)$$

$$F_{AFE} = -\frac{F_{VW}\alpha_{AFE}\left(\frac{R+1}{R}\right)}{\sin\theta_2\left(1+\frac{\cos\theta_2}{\sqrt{R^2-\sin^2\theta_2}}\right)}. \quad (14)$$

The value of the angle of axial force effect α_{AFE} is chosen using experimental data. The generalized equation is, therefore, a combination of the two forces, F_{VW} and F_{AFE}, which may be expressed as:

$$F = F_{VW} + F_{AFE}$$

$$= F_{VW}\left(1 - \frac{\alpha_{AFE}\left(\frac{R+1}{R}\right)}{\sin\theta_2\left(1 + \frac{\cos\theta_2}{\sqrt{R^2 - \sin^2\theta_2}}\right)}\right)$$

$$= \frac{k_1}{r_2}\Phi, \qquad (15)$$

$$\Phi = \left(\frac{R\cos\theta_3\left(\theta_{k1} + K_1\theta_{k2}\right) + \cos\theta_2\left(K_1\theta_{k2} + K_2\theta_{k3}\right)}{R\sin\left(\theta_2 - \theta_3\right)}\right)$$

$$\times\left(1 - \frac{\alpha_{AFE}\left(\frac{R+1}{R}\right)}{\sin\theta_2\left(1 + \frac{\cos\theta_2}{\sqrt{R^2 - \sin^2\theta_2}}\right)}\right), \qquad (16)$$

where:

$$\theta_3 = \sin^{-1}\left(-\frac{1}{R}\sin\theta_2\right), \qquad (17)$$

$$\theta_{k1} = \theta_2 = \cos^{-1}\left(\frac{r_1^2 + r_2^2 - r_3^2}{2r_1r_2}\right), \qquad (18)$$

$$\theta_{k2} = \theta_{k1} + \sin^{-1}\left(\frac{1}{R}\sin\theta_2\right), \qquad (19)$$

$$\theta_{k3} = \sin^{-1}\left(\frac{1}{R}\sin\theta_2\right). \qquad (20)$$

Equations (15) through (20) represent the generalized mathematical model (GMM) for all configurations of CFCSEC. A close examination shows that Eq. (16) is dimensionless and therefore F depends only on the non-dimensionalized parameter Φ, the spring constant k_1, and link length r_2. The spring constant is considered to be the stiffness parameter, while the link length is known as the geometric parameter. Thus, the creation of non-dimmensionalized parameter reduced the number of independent variables, making the model easier to use.

3. Results and Discussion

Table 4 gives the parameters and values for the CFCSECs for a 10% displacement. Maximum flexible segments parameter values for CFCSECs for a 20, 30 and 40% displacement are shown in Tables 5, 6, and 7, respectively. The variables *b*, *h*, and *I* are the width, thickness, and area moment of inertia of the flexible segment's cross section, and *E* is the modulus of elasticity of the rigid and flexible segments. Figure 4 shows the force displacement plots for a 10, 15, 20, and 25% displacement of the different CFCSECs. Figure 5 shows the percentage constant-force prediction plots as a function of time for a 10, 15, 20, and 25% displacement of the different CFCSECs. The results, as summarized in Table 8 for a 10, 15, 20, and 25% displacement and demonstrated clearly in Figs. 4 and 5, show that CFCSECs maintained substantially constant output force over the range of its input displacement. Such mechanisms can be configured in different ways to improve wire harness connections, improve docking station contact integrity, improve battery terminal performance, and improve rotor brush wear. CFCSECs will improve the performance of most electrical contacts.

4. Conclusion

New configurations that combine the benefits of both ECs and CCFMs were developed in this research work. The application of CCFM technology to ECs could provide a number of benefits in terms of performance, robustness, and package size. The development of these new configurations for use as CFCSECs promises to create new possibilities in ECs design and will go a long way in overcoming the challenges encountered in the implementation of the current traditional CCFM in ECs. The new class of CCFMs for use as CFCSECs has successfully eliminated all pin joints and has replaced them with short flexural pivots, and where these short flexural pivots exist, they only serve to mimic (simulate the behavior of) the local hinges.

Table 4. Parameters and values for CFCSECs for a 10% displacement.

Parameter	$Class\ 3A-lssm$	$Class\ 3A-slsm$	$Class\ 3A-llsm$	$Class\ 3A-lslm$
r_2	4.5165 mm	4.8077 mm	4.5699 mm	4.2757 mm
r_3	4.5165 mm	4.8077 mm	4.5699 mm	4.2757 mm
r_5	0.7631 mm	-	0. 6775 mm	0.7247 mm
r_6	-	-	-	0.7247 mm
m_2	0.0168 g	0.0166 g	0.0153 g	0.0158 g
m_3	0.0164 g	0.0166 g	0.0157 g	0.0158 g
m_S	4.3768 g	4.3768 g	4.3768 g	4.3768 g
b	5 mm	5 mm	5 mm	5 mm
h_{Solid}	0.1 mm	0.1 mm	0.1 mm	0.1 mm
h_1	0.0457 mm	0.0085 mm	0.0312 mm	0.0434 mm
h_2	0.0043 mm	0.0244 mm	0.0219 mm	0.0038 mm
h_3	0.0092 mm	0.0085 mm	0.0082 mm	0.0434 mm
I_1	3.9759×10^{-17} m^4	2.5254×10^{-19} m^4	1.2699×10^{-17} m^4	3.4046×10^{-17} m^4
I_2	3.2505×10^{-20} m^4	6.0503×10^{-18} m^4	4.3597×10^{-18} m^4	2.2205×10^{-20} m^4
I_3	3.2084×10^{-19} m^4	2.5254×10^{-19} m^4	2.2453×10^{-19} m^4	3.4046×10^{-17} m^4
E	110 GPa	110 GPa	110 GPa	110 GPa
S_Y	552 Mpa	552 Mpa	552 Mpa	552 Mpa
l_1	1.5263 mm	0.3803 mm	1.3551 mm	1.4494 mm
l_2	0.3840 mm	1.6297 mm	1.4611 mm	0.3382 mm
l_3	0.4119 mm	0.3803 mm	0.3657 mm	1.4494 mm
k_1	4.2599 mNm	0.1461 mNm	1.9905 mNm	3.8414 mNm
k_2	0.0186 mNm	0.6071 mNm	0.4880 mNm	0.0144 mNm
k_3	0.1714 mNm	0.1461 mNm	0.1351 mNm	3.8414 mNm
Mean Force	1.0163 N	0.5765 N	0.9090 N	1.8443 N
Parameter	$Class\ 3A-lllm$	$Class\ 3A-llsRig$	$Class\ 3A-lllFle$	$Class\ 3A-lllRig$
r_2	4.3478 mm	4.5528 mm	4.3478	4.3478 mm
r_3	4.3478 mm	4.5528 mm	4.3478 mm	4.3478 mm
r_5	0.6522 mm	0.6711 mm	0. 6319 mm	0.6319 mm
r_6	0.6522 mm	-	0.6319 mm	0.6319 mm
Rig	-	3.6215 mm	-	2.9487 mm
m_2	0.0143 g	0.0083 g	0.0060 g	0.0060 g
m_3	0.0143 g	0.0157 g	0.0060 g	0.0145 g
m_S	4.3768 g	4.3768 g	4.3768 g	4.3768 g
b	5 mm	5 mm	5 mm	5 mm
h_{Solid}	0.1 mm	0.1 mm	0.1 mm	0.1 mm
h_1	0.0301 mm	0.0232 mm	0.0177 mm	0.0177 mm
h_2	0.0150 mm	0.0232 mm	0.0177 mm	0.0177 mm
h_3	0.0301 mm	0.0081 mm	0.0177 mm	0.0291 mm
I_1	1.1326×10^{-17} m^4	5.2261×10^{-18} m^4	2.3053×10^{-18} m^4	2.3053×10^{-18} m^4
I_2	1.4158×10^{-18} m^4	5.2261×10^{-18} m^4	2.3053×10^{-18} m^4	2.3053×10^{-18} m^4
I_3	1.1326×10^{-17} m^4	2.1814×10^{-19} m^4	2.3053×10^{-18} m^4	1.0301×10^{-17} m^4
l_1	1.3043 mm	4.4740 mm	4.2124 mm	4.2124 mm
l_2	1.3043 mm	5.1736 mm	5.1151 mm	5.1151 mm
l_3	1.3043 mm	0.3622 mm	4.2124 mm	4.2124 mm
k_1	1.8443 mNm	0.8270 mNm	0.3875 mNm	0.3875 mNm
k_2	0.2305 mNm	0.5506 mNm	0.3191 mNm	0.3191 mNm
k_3	1.8443 mNm	0.1325 mNm	0.3875 mNm	1.7312 mNm
Mean Force	1.0803 N	0.7075 N	0.4806 N	0.7955 N

Table 5. Maximum flexible segments parameter values for CFCSECs for a 20% displacement.

Parameter	$Class\ 3A-lssm$	$Class\ 3A-slsm$	$Class\ 3A-llsm$	$Class\ 3A-lslm$
h_1	0.0320 mm	0.0059 mm	0.0219 mm	0.0304 mm
h_2	0.0030 mm	0.0171 mm	0.0153 mm	0.0026 mm
h_3	0.0064 mm	0.0059 mm	0.0057 mm	0.0304 mm
k_1	1.4668 mNm	0.0503 mNm	0.6854 mNm	1.3227 mNm
k_2	0.0064 mNm	0.2090 mNm	0.1680 mNm	0.0050 mNm
k_3	0.0590 mNm	0.0503 mNm	0.0465 mNm	1.3227 mNm
Mean Force	0.3568 N	0.2024 N	0.3191 N	0.6474 N
Parameter	$Class\ 3A-lllm$	$Class\ 3A-llsRig$	$Class\ 3A-lllFle$	$Class\ 3A-lllRig$
h_1	0.0211 mm	0.0163 mm	0.0124 mm	0.0124 mm
h_2	0.0105 mm	0.0163 mm	0.0124 mm	0.0124 mm
h_3	0.0211 mm	0.0056 mm	0.0124 mm	0.0204 mm
k_1	0.6350 mNm	0.2847 mNm	0.1334 mNm	0.1334 mNm
k_2	0.0794 mNm	0.1896 mNm	0.1099 mNm	0.1099 mNm
k_3	0.6350 mNm	0.0456 mNm	0.1334 mNm	0.5961 mNm
Mean Force	0.3793 N	0.2484 N	0.1687 N	0.2793 N

Table 6. Maximum flexible segments parameter values for CFCSECs for a 30% displacement.

Parameter	$Class\ 3A-lssm$	$Class\ 3A-slsm$	$Class\ 3A-llsm$	$Class\ 3A-lslm$
h_1	0.0259 mm	0.0048 mm	0.0177 mm	0.0246 mm
h_2	0.0024 mm	0.0138 mm	0.0124 mm	0.0021 mm
h_3	0.0052 mm	0.0048 mm	0.0046 mm	0.0246 mm
k_1	0.7767 mNm	0.0266 mNm	0.3629 mNm	0.7004 mNm
k_2	0.0034 mNm	0.1107 mNm	0.0890 mNm	0.0026 mNm
k_3	0.0312 mNm	0.0266 mNm	0.0246 mNm	0.7004 mNm
Mean Force	0.1928 N	0.1094 N	0.1724 N	0.3499 N
Parameter	$Class\ 3A-lllm$	$Class\ 3A-llsRig$	$Class\ 3A-lllFle$	$Class\ 3A-lllRig$
h_1	0.0170 mm	0.0132 mm	0.0100 mm	0.0100 mm
h_2	0.0085 mm	0.0132 mm	0.0100 mm	0.0100 mm
h_3	0.0170 mm	0.0046 mm	0.0100 mm	0.0165 mm
k_1	0.3363 mNm	0.1508 mNm	0.0706 mNm	0.0706 mNm
k_2	0.0420 mNm	0.1004 mNm	0.0582 mNm	0.0582 mNm
k_3	0.3363 mNm	0.0242 mNm	0.0706 mNm	0.3157 mNm
Mean Force	0.2049 N	0.1342 N	0.0912 N	0.1509 N

Table 7. Maximum flexible segments parameter values for CFCSECs for a 40% displacement.

Parameter	$Class\ 3A-lssm$	$Class\ 3A-slsm$	$Class\ 3A-llsm$	$Class\ 3A-lslm$
h_1	0.0222 mm	0.0041 mm	0.0152 mm	0.0211 mm
h_2	0.0021 mm	0.0119 mm	0.0106 mm	0.0018 mm
h_3	0.0045 mm	0.0041 mm	0.0040 mm	0.0211 mm
k_1	0.4902 mNm	0.0168 mNm	0.2290 mNm	0.4420 mNm
k_2	0.0021 mNm	0.0699 mNm	0.0561 mNm	0.0017 mNm
k_3	0.0197 mNm	0.0168 mNm	0.0155 mNm	0.4420 mNm
Mean Force	0.1243 N	0.0705 N	0.1112 N	0.2255 N
Parameter	$Class\ 3A-lllm$	$Class\ 3A-llsRig$	$Class\ 3A-lllFle$	$Class\ 3A-lllRig$
h_1	0.0146 mm	0.0113 mm	0.0086 mm	0.0086 mm
h_2	0.0073 mm	0.0113 mm	0.0086 mm	0.0086 mm
h_3	0.0146 mm	0.0039 mm	0.0086 mm	0.0142 mm
k_1	0.2122 mNm	0.0952 mNm	0.0446 mNm	0.0446 mNm
k_2	0.0265 mNm	0.0634 mNm	0.0367 mNm	0.0367 mNm
k_3	0.2122 mNm	0.0152 mNm	0.0446 mNm	0.1992 mNm
Mean Force	0.1321 N	0.0865 N	0.0588 N	0.0973 N

Table 8. Summary of results for a 10, 15, 20 and 25% displacement.

Configuration	*R*	PCF (%)	Mean F (N)	STDev (N)	PCF (%)	Mean F (N)	STDev (N)
		10% Displacement			15% Displacement		
Class $3A-lssm$	1.0	96.9681	1.0163	±0.0112	95.4269	0.5513	±0.0092
Class $3A-slsm$	1.0	96.9681	0.5765	±0.0063	95.4269	0.3127	±0.0052
Class $3A-llsm$	1.0	96.9681	0.9090	±0.0100	95.4269	0.4930	±0.0082
Class $3A-lslm$	1.0	96.9681	1.8443	±0.0203	95.4269	1.0004	±0.0167
Class $3A-lllm$	1.0	96.9681	1.0803	±0.0119	95.4269	0.5860	±0.0098
Class $3A-llsRig$	1.0	96.9681	0.7075	±0.0078	95.4269	0.3838	±0.0064
Class $3A-lllFle$	1.0	96.9681	0.4806	±0.0053	95.4269	0.2607	±0.0044
Class $3A-lllRig$	1.0	96.9681	0.7955	±0.0087	95.4269	0.4315	±0.0072
		20% Displacement			25% Displacement		
Class $3A-lssm$	1.0	93.8681	0.3568	±0.0081	92.2912	0.2544	±0.0073
Class $3A-slsm$	1.0	93.8681	0.2024	±0.0046	92.2912	0.1443	±0.0041
Class $3A-llsm$	1.0	93.8681	0.3191	±0.0072	92.2912	0.2275	±0.0065
Class $3A-lslm$	1.0	93.8681	0.6474	±0.0146	92.2912	0.4616	±0.0132
Class $3A-lllm$	1.0	93.8681	0.3793	±0.0086	92.2912	0.2704	±0.0077
Class $3A-llsRig$	1.0	93.8681	0.2484	±0.0056	92.2912	0.1771	±0.0051
Class $3A-lllFle$	1.0	93.8681	0.1687	±0.0038	92.2912	0.1203	±0.0034
Class $3A-lllRig$	1.0	93.8681	0.2793	±0.0063	92.2912	0.1991	±0.0057

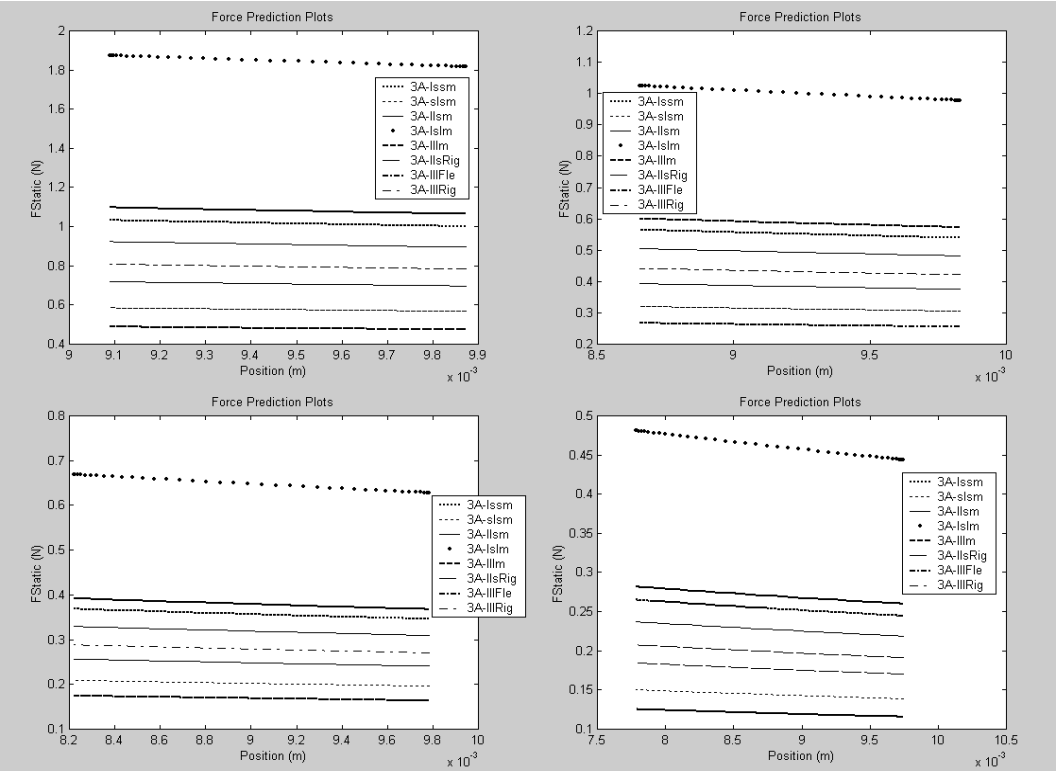

Fig. 4. Force displacement plots for a 10, 15, 20, and 25% displacement of the different CFCSECs.

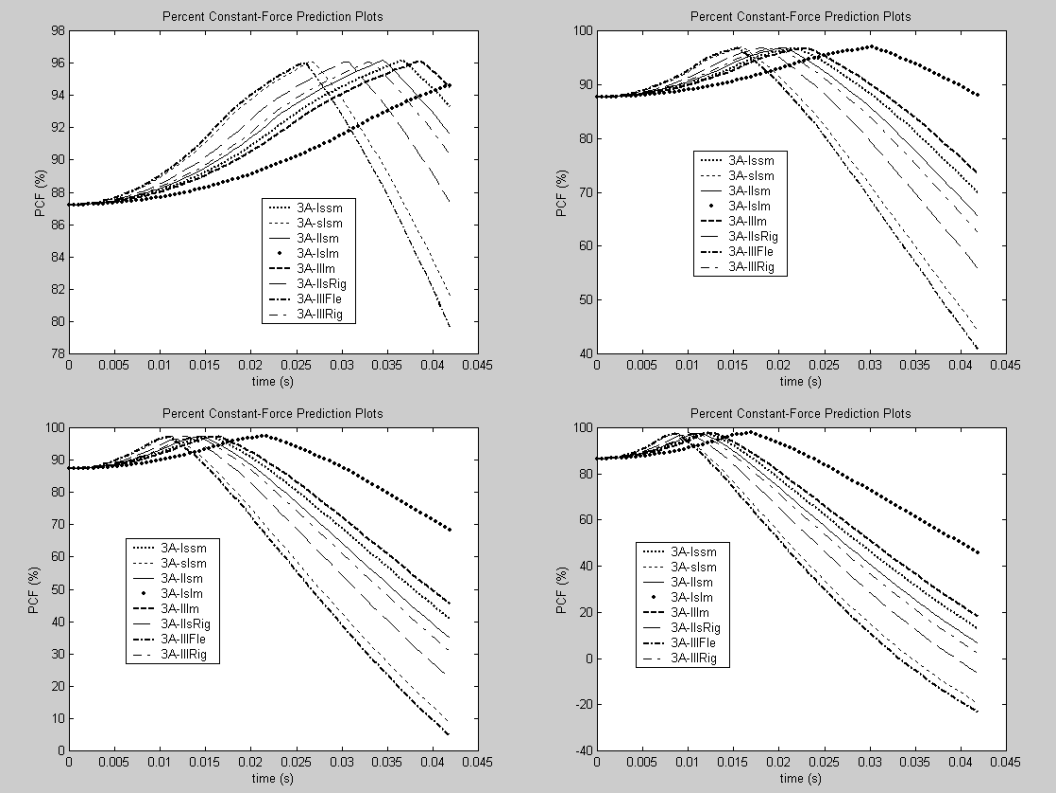

Fig. 5. Percent constant-force prediction plots as a function of time for a 10, 15, 20, and 25% displacement of the different CFCSECs.

The results obtained show that CFCSECs maintained substantially constant output force over the range of its input displacement. Such mechanisms can be configured in different ways to improve wire harness connections, docking station contact integrity, battery terminal performance, and rotor brush wear. CFCSECs will improve the performance of most electrical contacts.

References

Chen, L. 2001. Microfabrication of hetero-geneous, optimized compliant mechanisms. National Science Foundation (NSF) Summer Undergraduate Fellowship in Sensor Technologies (SUNFEST 2001), University of Rochester, Rochester, NY, USA, pp. 34-54.

Harper, C.A. 1996. Electronic packaging and interconnection handbook. 2nd ed., McGraw-Hill, New York, NY, USA.

Larsen, U.D.; Sigmund, O.; and Bouwstra, S. 1997. Design and fabrication of compliant micromechanisms and structures with negative Poisson's ratio. Journal of Microelectromechanical Systems 6(2): 99-106, June.

Millar, A.J.; Howell, L.L.; and Leonard, J.N. 1996. Design and evaluation of compliant constant-force mechanisms. Proc. American Society of Mechanical Engineers (ASME) 24th Biennial Mechanisms Conference, 18-22 August 1996, Irvine, CA, USA, 96-DETC/MECH-1209.

Mortensen, C.R.; Weight, B.L.; Howell, L.L.; and Magleby, S.P. 2000. Compliant mechanism prototyping. Proc. American Society of Mechanical Engineers (ASME) 26th Biennial Mechanisms and Robotics Conference, 10-13 September 2000, Baltimore, MD, USA, DETC2000/MECH-14204.

Sandor, G.N.; and Erdman, A.G. 1988. Advanced mechanism design: Analysis and synthesis. Prentice-Hall, New Delhi, India, vol. 2, pp. 435-530.

Weight, B.L. 2001. Development and design of constant-force mechanisms. Master's Thesis, Department of Mechanical Engineering, Brigham Young University, Provo, UT, USA.